plants

MDPI

Article

Diameter Class-Dependent Species-Specific Tree–Soil Feedback Linked to Soil Quality Between *Cunninghamia lanceolata* (Lamb.) Hook. and *Quercus fabri* Hance in Subtropical Forests

Gang Lei [1,2], Yang Yang [1,2], Wenting Li [1,2], Tian Chen [3] and Lianghua Qi [1,2,*]

[1] International Center for Bamboo and Rattan, Beijing 100102, China; leigang@icbr.ac.cn (G.L.); yangyang@icbr.ac.cn (Y.Y.); liwenting@icbr.ac.cn (W.L.)
[2] Sanya Research Base, International Center for Bamboo and Rattan, Sanya 572000, China
[3] College of Life and Environmental Sciences, Huangshan University, Huangshan 245041, China; chentianenci@caf.ac.cn
* Correspondence: qlh@icbr.ac.cn; Tel.: +86-010-8478-9733; Fax: +86-010-8478-9733

Abstract

The coupling between tree biomass and soil microhabitats is central to subtropical forest soil functioning, yet species- and stage-specific tree–soil interactions remain understudied. This study quantified these interactions in two dominant species—*Cunninghamia lanceolata* (Lamb.) Hook. (*C. lanceolata*) and *Quercus fabri* Hance (*Q. fabri*)—across five diameter at breast height (DBH) classes (5–10, 10–15, 15–20, 20–25, 25–30 cm). Soil quality was characterized via the Soil Quality Index (SQI) based on 16 physicochemical and enzyme activity parameters, while random forest models identified biomass importance. Soil properties and enzyme activities varied with diameter class ($p < 0.05$): *C. lanceolata* showed a unimodal pattern (minimum at 15–20 cm DBH), whereas *Q. fabri* increased consistently (peaking at 20–30 cm DBH). The diameter class × species interaction significantly influenced SQI ($p < 0.01$): *Q. fabri* showed higher SQI than *C. lanceolata* at larger DBH, and vice versa at smaller DBH. Aboveground biomass dominated SQI variation in *C. lanceolata* (weight = 0.57), whereas belowground biomass dominated in *Q. fabri* (weight = 0.52; model $R^2 > 0.75$). These findings demonstrate that DBH size and species identity jointly shape soil microenvironments, providing a mechanistic basis for informed subtropical forest management.

Keywords: tree–soil feedback; diameter classes; species-specific; soil quality index

Check for updates

Academic Editor: Josefa Lopez-Marin

Received: 15 December 2025
Revised: 21 January 2026
Accepted: 23 January 2026
Published: 28 January 2026

Copyright: © 2026 by the authors. Licensee MDPI, Basel, Switzerland. This article is an open access article distributed under the terms and conditions of the Creative Commons Attribution (CC BY) license.

1. Introduction

In forest ecosystems, trees do not exist in isolation but form dynamic co-evolutionary complexes with tree-influenced soil microhabitats [1,2]. Tree biomass, a key indicator of forest productivity and carbon sequestration, accumulates with growth traits such as diameter at breast height (DBH) and tree height, and is integral to this co-evolutionary process [3]. Traditional studies largely focused on unidirectional effects—either soil influencing trees or vice versa—whereas modern ecological theory highlights continuous bidirectional feedback between the two [4]. Soil physicochemical properties (e.g., nutrient pools, pH) and biochemical activities (e.g., enzyme activities) provide conditions for tree establishment, growth, and competition, acting as a filtering mechanism [5–8]. In turn, trees reshape soil microhabitats via canopy structure, litter inputs, and root exudates, engineering soil properties [9]. This bidirectional feedback drives spatial heterogeneity in

belowground processes. Feedback intensity and direction exhibit species specificity and stage dependency [10–12], suggesting tree species with distinct life history and resource use strategies have fundamentally different soil interaction mechanisms [13]. For example, across forest ecosystems in Hunan Province, vegetation type determined a distinct soil quality rank: shrubland > bamboo forest > broadleaved forest > conifer–broadleaved mixed forest > coniferous forest, attributed to intensifying stand competition [14]. In subtropical secondary forest restoration, evergreen coniferous, conifer–broadleaved mixed, and deciduous broadleaved stands differed in soil enzyme activities and microbial nutrient limitation: evergreens eased microbial P limitation, whereas deciduous broadleaved trees eased microbial C limitation, and pioneer/mid-successional deciduous species best balanced microbial nutrient demands [15]. As trees develop and DBH increases, dynamic shifts in biomass, morphology, and resource modification capacity alter tree–soil feedback [1]. Investigating the relationships among tree species, size, and soil microhabitat relationships at the individual level is critical for understanding forest co-evolutionary mechanisms. However, current vegetation–soil interaction research focuses on stand- or regional-scale analyses, homogenizing individuals of varying sizes and neglecting feedback driven by species identity and DBH class at the individual tree level [16–18]. Averaging such fine-scale variation risks obscuring key ecological processes. For functionally divergent, long-term coexisting tree species, species-specific feedback with soil microhabitats via abiotic pathways across growth stages remain critical research gaps.

Building on these gaps, this study selected two subtropical Chinese tree species—*Cunninghamia lanceolata* (Lamb.) Hook. (*C. lanceolata*) and *Quercus fabri* Hance (*Q. fabri*)—as focal taxa. *C. lanceolata* is a major timber species in China with high economic value and strong ecological adaptability [19]; *Q. fabri*—with an extensive root system and distinct litter decomposition traits—contributes significantly to ecosystem stability [20]. Adopting an individual-tree framework, this study compared tree-influenced soil microenvironment characteristics across diameter classes and quantified soil quality via the Soil Quality Index (SQI), integrating soil physicochemical properties (bulk density, pH, capillary/non-capillary porosity), nutrients (organic matter, total/available nitrogen and phosphorus), and enzyme activities (urease, peroxidase, acid phosphatase, and other hydrolases and oxidases). This study aimed to clarify how tree size and species identity jointly regulate soil microenvironments and biomass–soil quality coupling in subtropical plantations, thereby informing precision forest management. To address this overarching goal, three independent hypotheses were tested, corresponding to key questions about size effects, species effects, and biomass–soil coupling: (1) Soil microenvironments differ among conspecific individuals across diameter classes. (2) At equivalent sizes, *C. lanceolata* and *Q. fabri* form distinct soil microenvironments. (3) Species differ in biomass–SQI relationships.

2. Results

2.1. Analysis of Growth Characteristics of Forests Across Different Size Classes

Table 1 shows distinct population dynamics for *C. lanceolata* and *Q. fabri* across diameter classes. *C. lanceolata* exhibited a unimodal distribution: stem density peaked in Class III at 42 trees, then declined to 8 trees by Class V. *Q. fabri* showed a similar pattern, peaking at 30 trees in Class III and decreasing to 16 trees in Class V. These structural differences suggest divergent regeneration and survival strategies between the two species. Intra-class variability was low for *C. lanceolata*, with coefficients of variation (CV) under 50% for most growth parameters—diameter at breast height (DBH), tree height, and above- and belowground biomass—except belowground biomass in Class I, which reached 63.6%. Between-class variation was high for biomass, with CVs of 128.2% and 97.4% for aboveground and belowground components, respectively. This high between-class variation underscores strong

size-dependent effects on biomass accumulation. For *Q. fabri*, intra-class CVs were also below 50%, but between-class CVs were markedly higher (495.8% for aboveground biomass and 405.7% for belowground biomass), indicating greater size-dependent heterogeneity than that in *C. lanceolata*. Mean DBH for *C. lanceolata* increased from 2.1 to 17.8 cm between Class I and V, and aboveground biomass rose from 0.7 to 213.5 kg. *Q. fabri* exhibited a similar DBH increase (1.9 to 20.4 cm) but higher biomass accumulation (0.8 to 285.3 kg), confirming positive size-dependent growth.

Table 1. Descriptive statistics of forests in different classes.

Forests Type	Size Class	Number of Plants	Factor	Minimum	Maximum	Mean	Median	Standard Deviation	Coefficient of Variable (%)
C. lanceolata	I	25	DBH (cm)	1.98	2.49	2.08	2.20	0.35	16.83
			TH (m)	1.09	2.31	1.69	2.10	0.61	36.09
			AB (kg)	0.38	0.96	0.63	0.78	0.14	22.02
			BB (kg)	0.05	0.18	0.12	0.15	0.08	63.62
			TB (kg)	0.43	1.15	0.75	0.93	0.20	26.92
	II	30	DBH (cm)	4.01	4.71	4.37	4.50	0.30	6.86
			TH (m)	3.62	4.81	4.39	4.00	0.56	12.76
			AB (kg)	2.59	2.97	2.73	2.70	0.21	8.19
			BB (kg)	0.50	0.65	0.53	0.58	0.09	16.16
			TB (kg)	3.23	3.62	3.26	3.28	0.29	9.40
	III	42	DBH (cm)	5.20	7.31	6.42	6.50	0.79	12.31
			TH (m)	4.50	6.91	5.28	5.50	2.11	39.96
			AB (kg)	1.06	10.67	5.88	7.90	2.86	48.65
			BB (kg)	0.68	2.95	1.54	1.80	0.67	43.48
			TB (kg)	2.53	13.62	7.42	9.70	2.98	40.18
	IV	15	DBH (cm)	7.50	14.90	12.28	10.30	2.13	17.35
			TH (m)	5.10	14.20	8.37	11.50	2.26	27.00
			AB (kg)	9.31	55.07	31.59	43.60	12.24	38.74
			BB (kg)	2.24	12.28	7.86	9.80	2.88	36.68
			TB (kg)	11.55	67.35	39.45	53.40	14.95	37.89
	V	8	DBH (cm)	15.00	24.30	17.81	18.10	2.19	12.30
			TH (m)	7.10	17.50	12.48	14.20	2.77	22.20
			AB (kg)	46.80	153.03	77.54	123.10	25.31	32.64
			BB (kg)	11.51	38.27	18.18	22.10	5.70	31.37
			TB (kg)	58.32	191.29	95.73	145.20	30.78	32.15
	total	120	DBH (cm)	1.98	24.30	12.89	14.25	5.24	36.77
			TH (m)	1.09	17.50	9.08	9.25	3.90	42.14
			AB (kg)	0.38	153.03	44.01	25.29	32.43	128.24
			BB (kg)	0.05	38.27	10.54	7.66	7.45	97.37
			TB (kg)	0.43	191.29	54.55	32.95	39.88	122.76
Q. fabri	I	15	DBH (cm)	1.10	2.40	1.92	2.10	0.41	21.35
			TH (m)	1.50	2.90	2.14	2.05	0.45	21.03
			AB (kg)	0.38	1.05	0.67	0.70	0.19	28.58
			BB (kg)	0.08	0.49	0.30	0.25	0.14	47.62
			TB (kg)	0.46	1.55	0.97	1.06	0.33	33.66
	II	28	DBH (cm)	2.60	4.80	3.93	3.95	0.71	18.07
			TH (m)	2.90	4.20	3.59	3.55	0.39	10.86
			AB (kg)	1.21	3.32	2.31	1.98	1.16	50.40
			BB (kg)	0.58	2.93	1.78	1.77	0.89	49.79
			TB (kg)	1.80	6.25	4.10	3.75	1.98	48.33
	III	30	DBH (cm)	5.10	7.40	6.23	6.25	0.72	11.56
			TH (m)	4.90	8.10	6.60	6.90	0.97	14.70
			AB (kg)	7.96	20.32	14.49	16.89	3.36	23.21
			BB (kg)	3.13	7.55	4.92	4.12	1.24	25.29
			TB (kg)	14.20	27.08	19.41	21.01	4.48	23.10

Table 1. *Cont.*

Forests Type	Size Class	Number of Plants	Factor	Minimum	Maximum	Mean	Median	Standard Deviation	Coefficient of Variable (%)
Q. fabri	IV	31	DBH (cm)	7.90	14.90	10.53	10.30	1.95	18.52
			TH (m)	6.80	11.80	9.09	8.80	1.19	13.09
			AB (kg)	24.67	91.45	48.10	42.29	18.09	37.61
			BB (kg)	7.14	29.01	14.59	13.50	5.86	40.15
			TB (kg)	31.80	120.47	62.69	55.78	23.78	37.93
	V	16	DBH (cm)	17.60	22.30	20.37	20.10	1.67	8.20
			TH (m)	11.20	15.60	13.83	14.20	1.73	12.51
			AB (kg)	167.52	272.06	213.49	207.29	30.36	14.22
			BB (kg)	40.21	71.38	54.38	53.74	9.26	17.04
			TB (kg)	207.73	343.43	267.87	261.03	38.92	14.53
	total	120	DBH (cm)	1.10	22.30	7.77	5.85	5.64	96.39
			TH (m)	1.50	15.60	6.66	6.95	3.73	53.64
			AB (kg)	0.38	272.06	41.14	13.59	67.38	495.80
			BB (kg)	0.08	71.38	11.82	4.32	17.53	405.71
			TB (kg)	0.46	343.43	52.96	17.91	84.91	473.26

Note: DBH represents the diameter at breast height of trees; TH represents tree height; AB represents aboveground biomass; BB represents belowground biomass; and TB represents total biomass, the sum of aboveground biomass and belowground biomass. *Cunninghamia lanceolata* (Lamb.) Hook. (*C. lanceolata*) and *Quercus fabri* Hance (*Q. fabri*) were the two tree species investigated in this study.

2.2. Soil Factor Characteristics Across Size Classes

In *C. lanceolata* forests, bulk density and porosity did not vary among diameter classes, whereas Class III pH was lower than that of other classes ($p < 0.05$, Figure 1 and Table S2). Soil organic matter, total nitrogen, available nitrogen, peroxidase, and urease showed unimodal patterns with minima in Class III. These minima likely reflect intense nutrient uptake during peak growth in Class III. Dissolved organic carbon and available phosphorus were invariant among classes (Figures 2 and 3). Bulk density correlated negatively with urease, sucrase, and capillary porosity, while pH correlated positively with total nitrogen and most enzymes (Figure 3A). Soil organic matter correlated positively with total nitrogen and most enzymes but negatively with available P (Figure 3A). These relationships indicate tight coupling between soil physical properties, nutrient pools, and microbial functions in *C. lanceolata* stands.

In *Q. fabri* forests, bulk density and pH were unimodal: Class V bulk density exceeded Class I ($p < 0.05$) and Class V pH was lower than Class IV ($p < 0.05$). Non-capillary porosity remained stable, whereas Class I capillary porosity was lower than other classes ($p < 0.05$, Figure 1 and Table S2). Soil organic matter, total phosphorus, dissolved organic carbon and available nitrogen increased to peaks in Classes IV–V, while total N was unimodal with the highest value in Class V (Figure 2). Available phosphorus was lowest in Class IV (Figure 2 and Table S4). Bulk density correlated negatively with pH but positively with available nitrogen and most enzymes, while pH correlated positively with total nitrogen but negatively with total P and most enzymes (Figure 3B). Most enzyme activities were positively correlated (Figure 3B).

Interspecific comparisons revealed that forest type affected pH, capillary porosity, most nutrients, and urease and dehydrogenase activities (Figures 1–3). Diameter class influenced pH, soil organic matter, total phosphorus, peroxidase and acid phosphatase (Figures 1–3). Interactive effects were observed for pH, total nitrogen, total phosphorus and most enzymes (Figures 1–3). Across most classes, *C. lanceolata* forests had lower bulk density, pH, nutrients, sucrase and acid phosphatase than *Q. fabri* forests (Table S3). Conversely, dehydrogenase, Class II peroxidase and Class I nitrate reductase were lower in *Q. fabri* forests (Table S3).

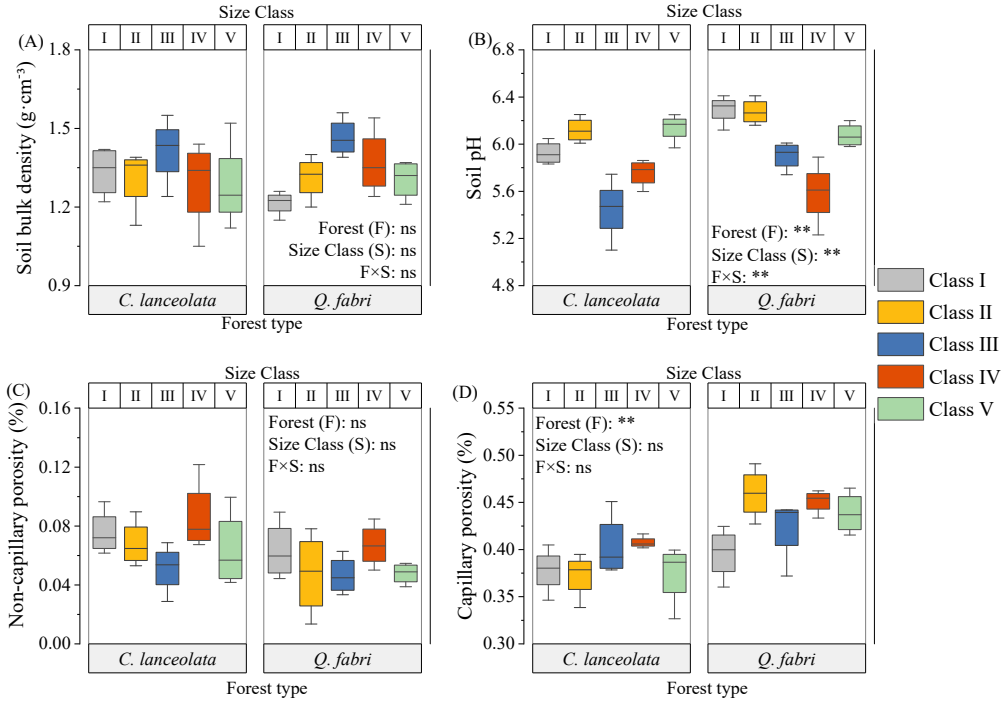


Figure 1. Soil physical and chemical properties across diameter classes in *C. lanceolata* and *Q. fabri* forests. Note: (**A**–**D**) show bulk density, pH, non-capillary porosity, and capillary porosity (means ± SE). Symbols *, **, and ns denote the significance of two-way ANOVA (forest type × size class) interactions: $p < 0.05$, $p < 0.01$, and non-significant, respectively. *Cunninghamia lanceolata* (Lamb.) Hook. (*C. lanceolata*) and *Quercus fabri* Hance (*Q. fabri*) were the two tree species investigated in this study.

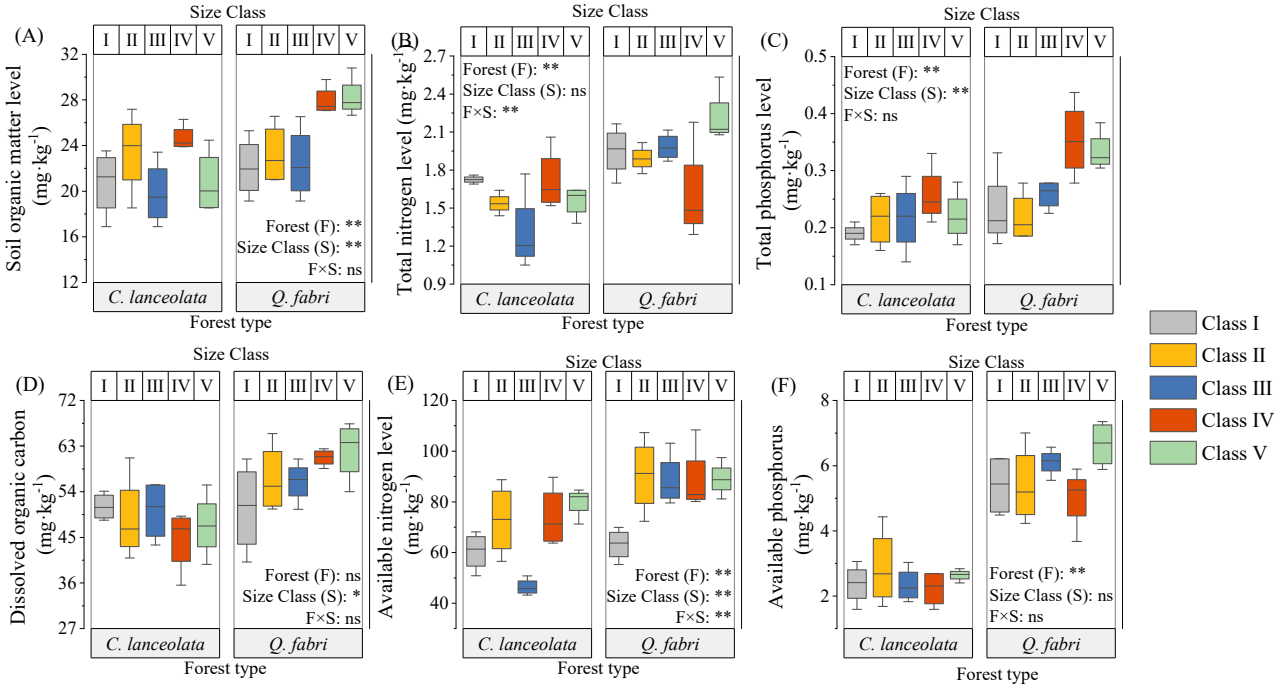


Figure 2. Differences in soil nutrient indicators across diameter classes in *C. lanceolata* and *Q. fabri* forests. Note: (**A**–**F**) represent soil organic matter, total nitrogen, total phosphorus, dissolved organic carbon, available nitrogen, and available phosphorus, respectively. Symbols *, **, and ns denote the significance of two-way ANOVA (forest type × size class) interactions: $p < 0.05$, $p < 0.01$, and non-significant, respectively. *Cunninghamia lanceolata* (Lamb.) Hook. (*C. lanceolata*) and *Quercus fabri* Hance (*Q. fabri*) were the two tree species investigated in this study.

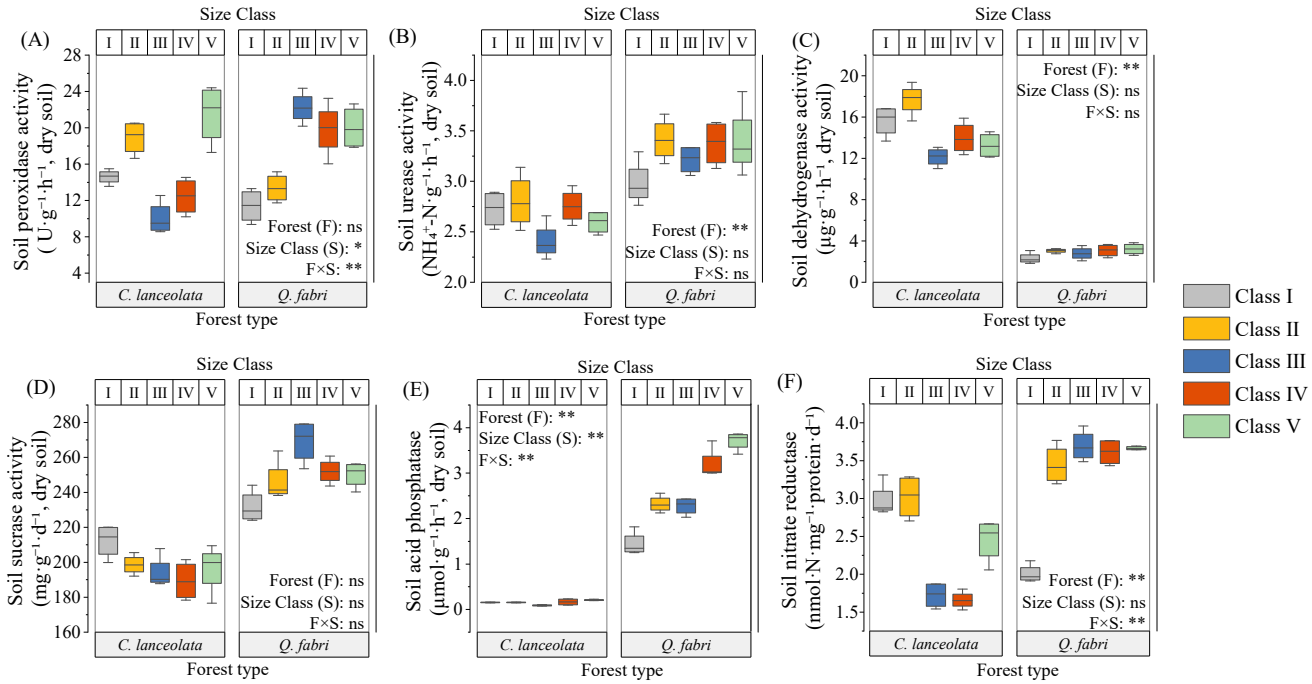
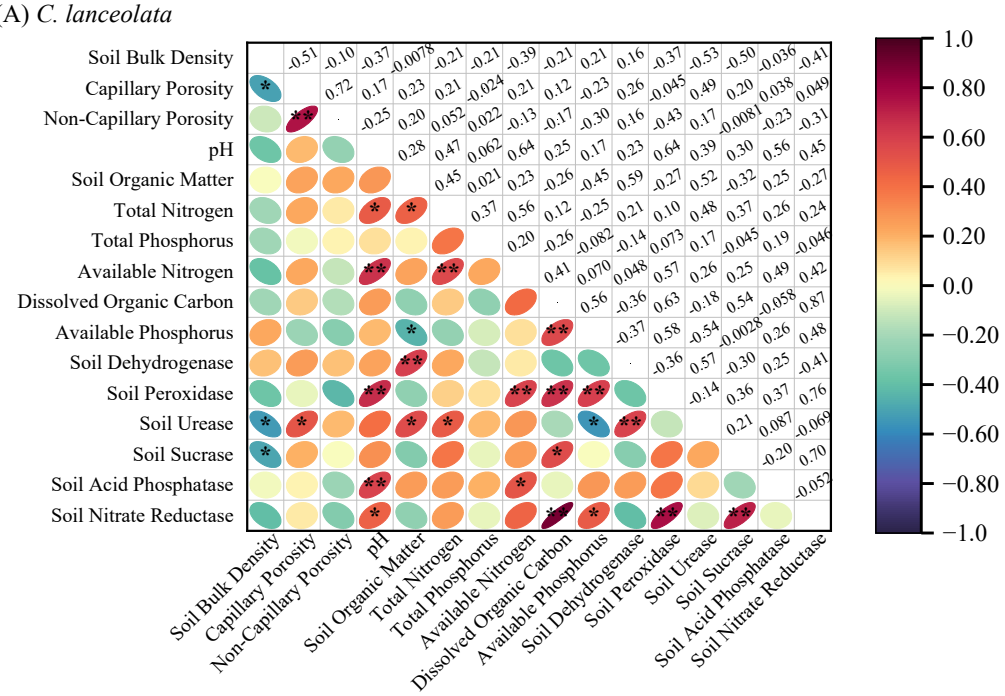


Figure 3. Differences in soil enzyme activities across diameter classes in *C. lanceolata* and *Q. fabri* forests. Note: (**A**–**F**) represent soil peroxidase, urease, dehydrogenase, sucrase, acid phosphatase, and nitrate reductase activities, respectively. Symbols *, **, and ns denote the significance of two-way ANOVA (forest type × size class) interactions: $p < 0.05$, $p < 0.01$, and non-significant, respectively. *Cunninghamia lanceolata* (Lamb.) Hook. (*C. lanceolata*) and *Quercus fabri* Hance (*Q. fabri*) were the two tree species investigated in this study.



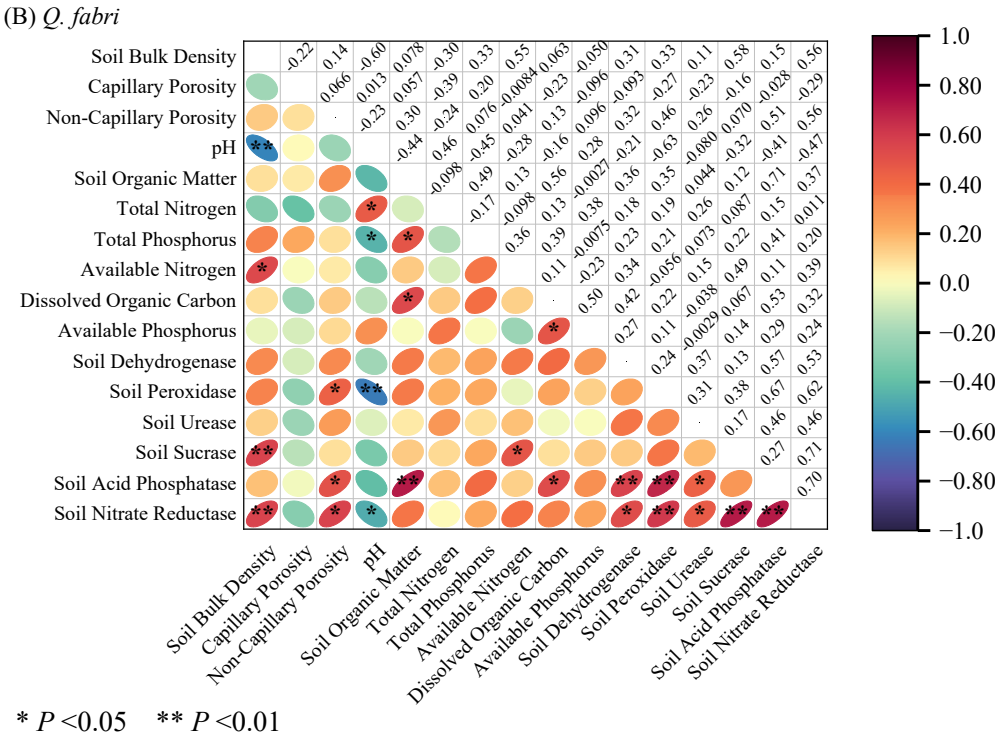


Figure 3. Correlation analysis of soil factor characteristics in *C. lanceolata* and *Q. fabri* forests. Note: (**A**,**B**) represent correlation networks for *C. lanceolata* and *Q. fabri* forests, respectively. ** and * denote significance at $p < 0.01$ and $p < 0.05$, respectively. *Cunninghamia lanceolata* (Lamb.) Hook. (*C. lanceolata*) and *Quercus fabri* Hance (*Q. fabri*) were the two tree species investigated in this study.

2.3. Soil Microhabitat Characteristics of Forests Across Different Size Classes

Principal component analysis (PCA) revealed distinct soil feature structures between *C. lanceolata* and *Q. fabri* forests. In *C. lanceolata*, five key components explained 81.2% of the total variance (Table 2). PC1 accounted for 27.5% of the variance and correlated strongly with pH, available nitrogen, and nitrate reductase activity, reflecting soil acidity and nitrogen availability. PC2 explained 24.5% of the variance and correlated with soil organic matter and urease activity, indicating organic matter supply capacity. PC3–PC5 each contributed <10% and were associated with bulk density, porosity, and phosphorus availability. These components indicate that *C. lanceolata* soils are primarily governed by pH–nitrogen interactions. In *Q. fabri*, six components explained 81.7% of the variance (Table 3). PC1 explained 32.0% of the variance and correlated with bulk density, acid phosphatase, and nitrate reductase activity, indicating soil structural properties and enzymatic activity. PC2 accounted for 15.1% of the variance and correlated with pH and available phosphorus, reflecting phosphorus availability. PC3–PC6 each contributed <10% and were linked to nitrogen cycling and porosity. In contrast, *Q. fabri* soils are dominated by bulk density–phosphorus relationships. These distinct PCA structures provide a multivariate foundation for understanding species-specific soil modification strategies.

PCA-derived SQI increased with diameter class in both forest types. In *C. lanceolata*, SQI rose from Class II to V, peaking in Class V ($p < 0.05$, Figure 4). Similarly, *Q. fabri* exhibited optimal soil microhabitats in Class V, with values higher than Class II ($p < 0.05$, Figure 4). Forest type did not affect SQI, whereas diameter class and the forest type × diameter class interaction had significant effects ($p < 0.001$, Figure 4). Specifically, *Q. fabri* Class V soils had higher quality than *C. lanceolata* Class V soils, whereas *C. lanceolata* Class I soils had slightly higher SQI than *Q. fabri* Class I soils. These results demonstrate that larger diameter classes support superior soil microhabitats.

Table 2. Principal component analysis results, factor loadings, communal variances, and indicator weights for *Cunninghamia lanceolata* (Lamb.) Hook. forests.

Indicator	PC1	PC2	PC3	PC4	PC5	Common Factor Variance	Weights
Soil Bulk Density	−0.51	−0.34	−0.48	0.02	0.30	0.70	6.26
Non-capillary Porosity	0.13	0.60	0.51	0.53	−0.20	0.95	6.68
Capillary Porosity	−0.37	0.45	0.51	0.47	−0.06	0.83	6.72
pH	0.76	0.34	−0.33	0.06	−0.04	0.80	6.34
Soil Organic Matter	−0.05	0.77	−0.30	−0.05	0.19	0.72	5.17
Total Nitrogen	0.46	0.55	0.04	−0.17	0.60	0.90	6.38
Total Phosphorus	−0.40	0.10	0.46	0.28	0.58	0.80	5.87
Available Nitrogen	0.69	0.40	−0.23	0.08	0.23	0.74	6.43
Dissolved Organic Carbon	0.65	−0.40	0.31	0.12	0.11	0.70	6.34
Available Phosphorus	0.32	−0.69	−0.23	0.49	0.04	0.87	6.54
Dehydrogenase	−0.10	0.70	−0.38	−0.02	−0.21	0.68	5.33
Peroxidase	0.84	−0.34	−0.15	0.19	−0.05	0.88	6.43
Urease	0.34	0.82	0.17	−0.18	−0.16	0.87	6.53
Sucrase	0.62	−0.06	0.57	−0.34	−0.08	0.83	6.08
Acid Phosphatase	0.39	0.23	−0.70	0.36	−0.04	0.82	6.15
Nitrate Reductase	0.82	−0.35	0.31	−0.08	0.08	0.90	6.75
Eigen values	4.40	3.93	2.45	1.19	1.02		
Variance contribution	27.49	24.53	15.34	7.44	6.40		
Cumulative variance Contribution	27.49	52.02	67.36	74.80	81.20		

Note: PC1–PC5 represent the loadings of soil factors on the first five principal component axes.

Table 3. Principal component analysis results, factor loadings, communal variances, and indicator weights for *Quercus fabri* Hance forests.

Indicator	PC1	PC2	PC3	PC4	PC5	PC6	Common Factor Variance	Weights
Soil Bulk Density	0.59	−0.49	−0.41	0.18	−0.12	0.17	0.83	6.93
Non-capillary Porosity	−0.20	−0.35	0.55	−0.03	0.40	0.27	0.70	5.46
Capillary Porosity	0.52	0.04	0.20	−0.54	0.22	0.40	0.82	6.15
pH	−0.65	0.55	−0.11	0.17	0.32	0.16	0.89	6.95
Soil Organic Matter	0.62	0.01	0.58	0.08	−0.07	−0.24	0.79	5.74
Total Nitrogen	−0.01	0.77	−0.33	0.17	0.02	−0.31	0.83	4.83
Total Phosphorus	0.51	−0.29	0.38	0.38	0.04	−0.24	0.70	6.30
Available Nitrogen	0.43	−0.44	−0.31	0.46	0.40	−0.07	0.85	6.86
Dissolved Organic Carbon	0.51	0.38	0.40	0.47	−0.21	0.02	0.83	6.81
Available Phosphorus	0.19	0.68	0.05	0.30	−0.12	0.53	0.88	5.64
Dehydrogenase	0.63	0.25	0.04	0.17	0.44	0.02	0.68	5.61
Peroxidase	0.71	0.14	−0.06	−0.43	−0.40	−0.11	0.88	6.47
Urease	0.42	0.25	−0.33	−0.34	0.48	−0.34	0.81	6.73
Sucrase	0.57	−0.18	−0.51	0.21	−0.13	0.21	0.73	6.30
Acid Phosphatase	0.84	0.30	0.29	−0.15	0.09	−0.09	0.92	6.89
Nitrate Reductase	0.89	0.06	−0.28	−0.12	0.04	0.22	0.94	6.34
Eigen values	5.12	2.42	1.90	1.46	1.15	1.02		
Variance contribution	32.02	15.10	11.88	9.13	7.18	6.36		
Cumulative variance Contribution	32.02	47.13	59.01	68.14	75.32	81.68		

Note: PC1–PC6 represent the loadings of soil factors on the first six principal component axes.

Principal coordinate analysis (PCoA) of *C. lanceolata* soils showed that PCoA1 and PCoA2 explained 56.2% and 25.9% of the variance, respectively (82.1% cumulative; Figure 5A). These axes captured core differences in soil properties, with Class III samples clearly separated from other classes. This separation indicates that Class III represents a distinct soil microenvironment phase in *C. lanceolata* development. In *Q. fabri* forests, PCoA1 and PCoA2 explained 54.0% and 25.4% of the variance (79.4% cumulative; Figure 5B), and Class I samples were distinctly separated from other classes. Early-stage separation in *Q. fabri* suggests that this species establishes distinct soil conditions from the sapling stage. Thus, diameter class drove soil property differentiation in both forest types, but with different thresholds: *C. lanceolata* showed a mid-stage transition (Class III), whereas *Q. fabri* exhibited early differentiation followed by stabilization (Class I).

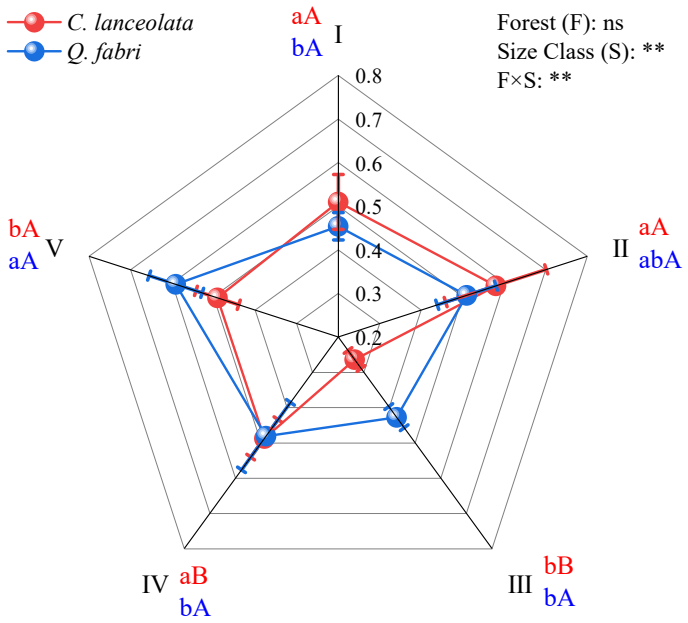


Figure 4. Differences in soil quality index across diameter classes in *C. lanceolata* and *Q. fabri* forests. Note: Within species, different lowercase letters indicate significant differences among DBH classes ($p < 0.05$); between species at the same DBH class, different uppercase letters indicate significant differences ($p < 0.05$). Symbols *, **, and ns denote the significance of two-way ANOVA (forest type × size class) interactions: $p < 0.05$, $p < 0.01$, and non-significant, respectively. *Cunninghamia lanceolata* (Lamb.) Hook. (*C. lanceolata*) and *Quercus fabri* Hance (*Q. fabri*) were the two tree species investigated in this study.

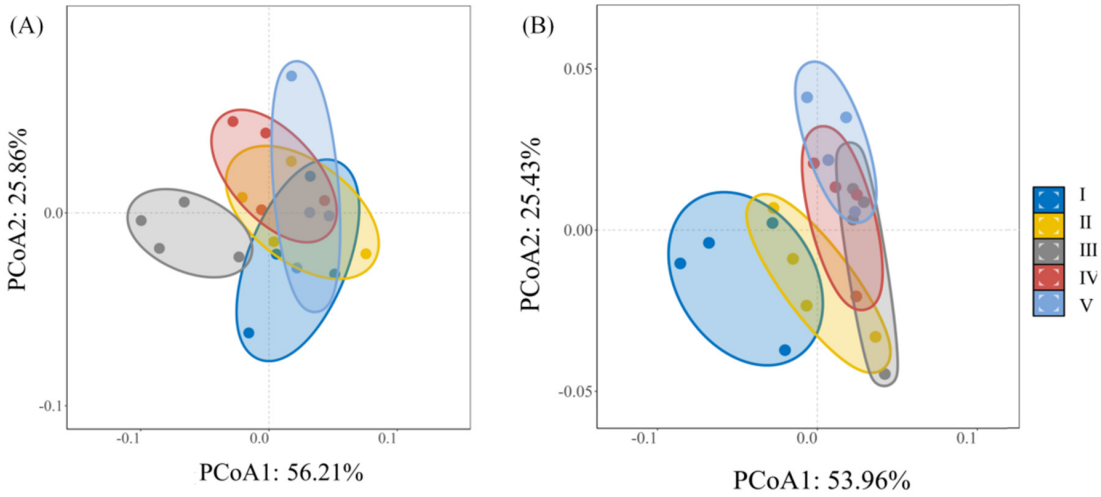


Figure 5. Principal coordinate analysis (PCoA) of soil factors in *Cunninghamia lanceolata* (Lamb.) Hook. (**A**) and *Quercus fabri* Hance (**B**) forest.

2.4. Differential Effects of Forest Biomass Types on Soil Quality Index

Using random forest models with SQI as the dependent variable, the importance of aboveground and belowground biomass in predicting soil quality for *C. lanceolata* and *Q. fabri* was quantified (Figure 6). The two species exhibited contrasting biomass–soil quality relationships: aboveground biomass was the primary driver for *C. lanceolata* (feature weight: 57% of variance explained), whereas belowground biomass dominated for *Q. fabri* (feature weight: 52%). Model performance was robust, with training R^2 values of 0.811 and 0.879 for *C. lanceolata* and *Q. fabri*, respectively, and testing $R^2 > 0.75$ for both species (low MAE and MSE). These findings confirm that random forest models effectively

capture nonlinear biomass–soil quality associations, revealing species-specific regulation: *C. lanceolata* relies primarily on aboveground processes, while *Q. fabri* depends more on belowground processes.

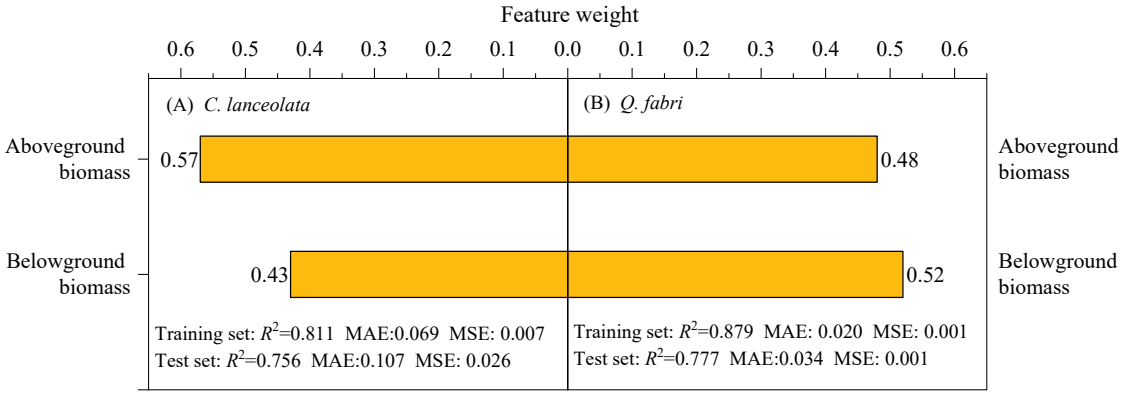


Figure 6. Feature weights of aboveground and belowground biomass on soil quality index from random forest analysis. Note: (**A**) *Cunninghamia lanceolata* (Lamb.) Hook. and (**B**) *Quercus fabri*. Hance MAE = mean absolute error; MSE = mean squared error.

3. Discussion

3.1. Species-Specific Diameter Class-Dependent Tree–Soil Interactions

This study documents differences in diameter class structure between *C. lanceolata* and *Q. fabri*, relating to divergent ecological strategies associated with species-specific niche differentiation. *C. lanceolata* had greater abundance in Class I (21% of the total) and its abundance peaked at Class III (35% of the total), whereas *Q. fabri* showed a different pattern at Class I and Class III (12.5% and 25% of the total, respectively). Table 1 visualizes these patterns, showing *C. lanceolata*'s higher Class I recruitment and Class III dominance versus *Q. fabri*'s lower initial recruitment. This pattern in *C. lanceolata* is consistent with cohort-driven regeneration following disturbance. Such post-disturbance regeneration directly impacts soil legacies through rapid litter and root inputs. In contrast, *Q. fabri* displayed a unimodal diameter class distribution, with mean DBH in Class V larger than that of *C. lanceolata* (20.37 vs. 17.81 cm). This pattern is associated with delayed maturation under closed-canopy conditions (Table 1). Delayed maturation allows *Q. fabri* to accumulate belowground biomass, intensifying root–soil interactions. Such size-dependent structural divergence directly impacts soil development trajectories, as larger trees intensify belowground resource partitioning. These diameter class distribution patterns are consistent with previously reported interspecific differences in shade tolerance and light acquisition strategies [21–23].

Soil physicochemical properties and enzyme activities varied significantly across diameter classes within each species (Figures 1–3), supporting Hypothesis 1. These variations underscore that size-dependent growth stages actively engineer soil conditions rather than passively reflecting them. For *C. lanceolata*, soil organic matter (SOM), total nitrogen (TN), and most enzyme activities followed a decline-then-rise trajectory, with minima at Class III—the stage of most rapid aboveground growth (Figures 2 and 3, Tables S3 and S4). These minima in Class III reflect peak nutrient demand during active growth. This pattern aligns with the growth–nutrient demand–litter feedback mechanism [24]: intense nutrient uptake during stem elongation is associated with transient soil nutrient depletion [25], which is subsequently mitigated by increased litter input as trees mature. These distribution patterns reveal species-specific regeneration strategies that differentially influence soil legacy development. Table 1 corroborates this interpretation, showing a threefold biomass increase from Class III to V that drives organic matter recovery. Aboveground

biomass nearly tripled from Class III to Class V (from ~68.2 kg to ~213.49 kg; Table 1), linked to recovery of SOM through decomposition processes [19]. This biomass-driven organic matter recovery is visually evident in Figure 2A, where SOM rises after Class III. Concurrently, soils in Class III had a significantly lower pH (Figure 2B), a pattern potentially linked to exudation of organic acids by roots—an established strategy for nutrient mobilization [26,27]. These findings collectively demonstrate that *C. lanceolata* actively modifies its soil microenvironment through size-dependent resource allocation. In contrast, *Q. fabri* displayed distinct soil dynamics: bulk density initially increased then declined, pH decreased before rising again, and key soil nutrients generally increased, with peak values observed in Classes IV–V (Figures 1 and 2, Tables S2 and S4). *Q. fabri* shows a different temporal pattern than *C. lanceolata*. These trends align with characteristics of its broadleaf litter, including a lower C:N ratio [28,29]—a trait associated with enhanced decomposability and more efficient nutrient cycling [30]. PCoA revealed that *Q. fabri* in Class I formed a distinct cluster (Figure 5B). This pattern is indicative of early-stage tree-influenced soil microenvironment specialization. This differs from *P. sylvestris*, where microhabitats of juvenile trees are minimally influenced by adult individuals [31]. Such ontogenetic shifts have direct management implications: retaining large-diameter trees sustains soil legacies, while species selection should consider these divergent temporal dynamics.

The significant species × diameter class interaction effect on soil parameters (Figures 1–3) provides empirical support for Hypothesis 2. This interaction effect demonstrates that species effects are size-dependent, not fixed, reinforcing the need for diameter class-based management. Cross-species comparisons at equivalent diameter classes showed that *C. lanceolata* stands had lower bulk density, pH, sucrase activity and acid phosphatase activity than *Q. fabri* stands (Figure 1), while dehydrogenase activity was lower in *Q. fabri* stands (Figure 3), reflecting fundamental differences in coniferous versus broadleaf litter and root traits. These trait-mediated mechanisms, illustrated by the contrasting soil chemistry in Figure 2, provide a mechanistic basis for species-specific fertilizer prescriptions. These differences relate to divergent litter chemistry: slow-decomposing needle litter of *C. lanceolata* is linked to long-term soil acidification [32], whereas labile leaf litter of *Q. fabri* associates with enhanced microbial activity. SQI analysis revealed no main effect of forest type, but a significant species × diameter class interaction ($p < 0.01$; Figure 4), which shows divergent SQI trajectories between the two species across diameter classes, confirming that species effects are size-dependent and reinforcing diameter class-based management. In Class V, *Q. fabri* stands had higher SQI than *C. lanceolata* stands, while *C. lanceolata* had slightly higher SQI than *Q. fabri* in Class I (Figure 4). This observation is consistent with Obade and Lal [33], who asserted that soil quality is shaped by biological traits and environmental context, and it highlights diameter class as a regulatory mediator of tree–soil interactions. These SQI patterns provide a quantitative basis for identifying low-quality stands: Class III *C. lanceolata* and Class I *Q. fabri* represent priority intervention zones. These findings are supported by additional data: the ordination plot in Figure 5A shows distinct clustering of Class III *C. lanceolata* samples, indicating a unique soil condition at this diameter class. Similarly, Class I *Q. fabri* samples formed a separate cluster (Figure 5B), suggesting early divergence in soil properties.

3.2. Diameter Class-Mediated Species Differences in Biomass–Soil Quality Coupling

Random forest analysis supported Hypothesis 3, delineating interspecific differences in biomass-driven SQI variation (Figure 6). The tree–soil relationship is not passive but dynamic and species-specific, with biomass and soil conditions mutually shaping each other. This feedback specificity reflects species-specific resource allocation and functional traits. For *C. lanceolata*, aboveground biomass weight was 0.57 and belowground biomass

0.43 in explaining SQI variation (Figure 6A). This aligns with coniferous strategies: *C. lanceolata* prioritizes vertical growth with a high shoot-to-root ratio [23]. It allocates more resources to xylem formation to compensate for tracheids' low water transport efficiency, with leaves of low N/P and high C content—emphasizing structural investment over rapid nutrient turnover [34]. Global conifer tree-ring data further confirm a widespread "fast growth–drought tolerance" trade-off [35]. This trade-off is embodied in the conservative growth strategy of *C. lanceolata*, which enhances environmental adaptability via structural resource investment. Conifer–broadleaf mixed forest studies support this stable growth strategy: *C. lanceolata*'s self-thinning trajectory matches that of pure stands, remaining within core thresholds without mixed-environment interference [36]. Higher aboveground biomass correlates with greater litter input, which indirectly modifies soil quality via decomposition, potentially forming a positive feedback loop.

Q. fabri showed the opposite pattern: belowground biomass contributed 52% to SQI variation versus 48% for aboveground biomass (Figure 6B). This aligns with broadleaf root traits: *Q. fabri* has a high fine root turnover rate, accelerating N/P release during decomposition [37]. Additionally, root-secreted organic acids convert soil P from stable to active forms via acidolysis, significantly improving P availability [38]. These processes form a dominant "belowground biomass–root processes–soil quality" pathway, consistent with the findings of Tedersoo et al. [39] and Norris et al. [40], who concluded that root–microbe interactions govern nutrient cycling in broadleaf forests. Furthermore, *Q. fabri* soil bacteria exhibit greater drought tolerance, while moderate shading elevates soil fungal diversity, strengthening belowground nutrient cycling stability [23]. These interspecific differences align with the "fast–slow continuum" framework: *C. lanceolata* (conifer) employs a "slow strategy" centered on structural investment and environmental adaptability, whereas *Q. fabri* (broadleaf) adopts a "resource-acquisitive strategy" focused on efficient nutrient turnover. This conclusion aligns with Shen et al. [14], who documented distinct biomass–soil coupling patterns across species with divergent life-history strategies in *P. massoniana* forests, further validating the generality of conifer-broadleaf feedback pathway differentiation reported herein.

Subtropical forest research indicates that conifers exhibit lower N resorption efficiency, greater seasonal fluctuations, and weaker disturbance resistance than broadleaves [41]. Plant–microbe interactions mediate these strategies: plants recruit specific soil microbes via chemical signals to enhance nutrient acquisition [42], while mycorrhizal fungi decompose organic matter and modulate nutrient fluxes through underground hyphal networks [39]. These microbial mechanisms, illustrated in our enzyme activity data (Figure 3), explain the functional differences observed between species. *C. lanceolata* relies on aboveground litter to regulate SQI; disturbances reduce litter quantity and quality and decomposition rate, impacting nutrient supplementation. In contrast, *Q. fabri* soil microenvironment feedback depends on root–microbe interactions, maintaining stability under moderate disturbances [43]. While random forest models revealed key patterns, they do not establish causal relationships in this study. This limitation is acknowledged in Figure 6, which shows correlation, not causation, between biomass and SQI. Future research should combine isotope tracing and time-series monitoring to verify biomass-soil feedback directionality, and incorporate mycorrhizal indicators to improve model explanatory power. This analytical framework (diameter class dynamics × species functional traits) advances mechanistic understanding of tree-soil interactions in subtropical forest ecosystems.

4. Materials and Methods

4.1. Study Area Overview

The study site (109°35′12″ E, 26°51′59″ N) lies in Moshao Village, Guangping Town, Huaihua, Hunan, China. Huitong County, in southwestern Hunan Province, lies within the mountainous region bordering the Yunnan–Guizhou Plateau–Jiangnan Hills transition zone the county is a core production area for *C. lanceolata*. The climate is subtropical monsoonal, with distinct wet–hot seasons. Mean annual temperature is 16.8 °C (January 4.8 °C, July 26.7 °C); 70% of the 1100–1400 mm annual precipitation falls during June–September, when monthly mean temperature exceeds 22 °C. Mean annual relative humidity is >80%. Soils are classified as loamy sand Luvisols (World Reference Base for Soil Resources, WRB) with a depth of approximately 40 cm. The specific study site is a hillside forestland with a southeast-facing aspect, a slope gradient of 40–57°, and an elevation range of 430–470 m.

4.2. Methodology

4.2.1. Plot Selection and Field Survey

The selected forests were pure stands of *C. lanceolata* and *Q. fabri* established in 1999 following clear-cutting in the autumn of 1998. Since afforestation, stands have received uniform management without silvicultural interventions (e.g., thinning). The understory shrub layer is dominated by *Maesa japonica* (Thunb.) Moritzi., *Oreocnide frutescens* (Thunb.) Miq., *Schima superba* Gardn. et Champ., etc. The understory herbaceous layer mainly consists of *Woodwardia japonica* (L.f.) Sm., *Parathelypteris glanduligera* (Kunze) Ching., *Carex doniana* Spreng., *Lophatherum gracile* Brongn., etc. In August 2024, four 20 m × 20 m plots were established per species (eight plots total; Section 4.1). Plots were located in 25-year-old plantations with inter-plot spacing ≥20 m. Stand density was 750–800 stems·hm^{-2} for *C. lanceolata* and 550–650 stems·hm^{-2} for *Q. fabri*. Elevation was controlled during plot selection to ensure similar topography and community structure, minimizing external environmental interference. To ensure the reliability and representativeness of the data, all living trees with a diameter at breast height (DBH, measured at 1.3 m above ground) of ≥1 cm within each plot were identified and measured. To guarantee consistency and comparability across species, a proportional stratified random sampling method was employed, with 120 trees selected per species for detailed analysis. The specific stratification method is detailed in Section 4.2.2.

4.2.2. Diameter Class Categorization and Biomass Calculation for Trees

Because DBH class reliably reflects tree developmental stage [44,45], all surveyed *C. lanceolata* and *Q. fabri* individuals were divided into five size classes: Class I: 1 cm < DBH ≤ 2.5 cm; Class II: 2.5 cm < DBH ≤ 5 cm; Class III: 5 cm < DBH ≤ 7.5 cm; Class IV: 7.5 cm < DBH ≤ 15 cm; Class V: 15 cm < DBH ≤ 30 cm [45]. The sampling ratio for each DBH class was determined according to its proportion in the total tree population of the corresponding stand. For example, if Class I accounted for 10% of the total population, then 12 trees from Class I were selected to be part of the 120 samples. This design ensured that the DBH class distribution of the selected sample was consistent with that of the entire plot. Compared to simple random sampling, this strategy effectively minimized potential biases and guaranteed that trees at different developmental stages were adequately and proportionally represented in the subsequent analysis. Biomass was calculated using allometric equations from the Chinese National Standard GB/T 43648–2024 [46]. The formula is as follows:

(1) Binary model for aboveground biomass:

$$M_A = a_0 \times DBH^{a_1} \times H^{a_2} \quad (1)$$

where M_A = aboveground biomass (kg), DBH = diameter at breast height (cm), H = tree height (m), and a_0, a_1, a_2 = species-specific parameters from GB/T 43648–2024 [46]. Parameter values are provided in Table 4.

(2) Binary model for belowground biomass:

$$M_B = b_0 \times DBH^{b_1} \times H^{b_2} \quad (2)$$

where M_B = belowground biomass (kg), DBH = diameter at breast height (cm), H = tree height (m), and b_0, b_1, b_2 = species-specific parameters from GB/T 43648–2024 [46]. Parameter values are provided in Table 5.

(3) Calculation Formula for Total Biomass:

$$M_T = M_A + M_B \quad (3)$$

Table 4. Binary allometric parameters for aboveground biomass estimation of *Cunninghamia lanceolata (Lamb.)* Hook. and *Quercus fabri* Hance in Hunan Province.

Forests Type	Diameter at Breast Height Range	Parameter Types	a_0	a_1	a_2
C. lanceolata	DBH ≥ 5.0 cm	Binary	0.06539	2.01735	0.49425
Q. fabri		Binary	0.13188	1.82892	0.71119
C. lanceolata	DBH < 5.0 cm	Binary	0.19071	1.35226	0.49425
Q. fabri		Binary	0.15444	1.73082	0.71119

Table 5. Binary allometric parameters for belowground biomass estimation of *Cunninghamia lanceolata (Lamb.)* Hook. and *Quercus fabri* Hance in Hunan Province.

Forests Type	Diameter at Breast Height Range	Parameter Types	b_0	b_1	b_2
C. lanceolata	DBH ≥ 5.0 cm	Binary	0.016385	2.52941	−0.11744
Q. fabri		Binary	0.114600	2.09235	−0.05245
C. lanceolata	DBH < 5.0 cm	Binary	0.034655	2.06398	−0.11744
Q. fabri		Binary	0.053436	2.56640	−0.05245

4.2.3. Soil Sample Collection and Soil Microhabitat Characterization

To ensure soil samples represented tree soil microhabitats, four soil blocks (10 cm × 10 cm × 20 cm) were excavated at the four cardinal points 1.5 m from each tree base and homogenized into one composite sample [1]. Prior to sampling, surface debris was removed. A subsample of each composite soil was passed through a 2 mm sieve, flash-frozen in liquid nitrogen, and stored at −20 °C for enzyme assays within one week. The remaining samples were transported to the laboratory, where they were air-dried, sieved (2 mm and 0.25 mm), and cleared of stones and root residues. Soil physicochemical properties—including bulk density (BD), capillary/non-capillary porosity, pH, soil organic matter (SOM), total nitrogen (TN), total phosphorus (TP), dissolved organic carbon (DOC), available nitrogen (AN), and available phosphorus (AP)—were analyzed following *Soil Agricultural Chemistry Analysis* (3rd ed.) [47]. Measured soil enzyme activities included peroxidase [48], dehydrogenase [49], urease [50], sucrase [51], acid phosphatase [52], and nitrate reductase [53].

Soil quality integrates physicochemical properties and ecosystem functionality. Therefore, the soil quality index (SQI) was used to evaluate soil microhabitats [1,54]. SQI was calculated via the Total Data Set (TDS) method in four steps [14]: (1) Averaging indicators, (2) Normalizing indicators, (3) Scoring indicators using correlation functions [55,56], and

(4) Integrating scored values into a final index. For pH, given that all soils were acidic (pH < 7.0), a "higher-the-better" rule was applied reflecting proximity to neutrality (optimum 7.0). Parameters classified as "higher-the-better" (SOM, TN, TP, DOC, AN, AP) were scored accordingly. Enzymes involved in nutrient cycling (dehydrogenase, urease, sucrase, acid phosphatase) were also classified as "higher-the-better". Peroxidase and nitrate reductase were classified as "lower-the-better" [57]. Specific equations are:

$$Q = \frac{X - Xmin}{Xmax - Xmin} \quad (4)$$

$$Q = \frac{Xmax - X}{Xmax - Xmin} \quad (5)$$

Here, Q denotes the membership degree (ranging from 0 to 1), X is the measured value of the indicator, X_{min} is the minimum value, and X_{max} is the maximum value of each indicator. Equation (4) was used for "higher-the-better" indicators, and Equation (5) for "lower-the-better" indicators. Principal component analysis (PCA) was subsequently performed on all soil indicators. Communal variances derived from PCA reflect the contribution of each indicator to the total variance, with larger values indicating greater importance [58]. Indicator weights were calculated from the PCA results using Equation (6), where *Ci* represents the absolute communal variance of indicator *i*.

$$W_i = \frac{Ci}{\sum_{i=1}^{n} Ci} \quad (6)$$

Finally, SQI under each forest stand was calculated based on the aforementioned Equation (7):

$$SQI = \sum_{i=1}^{n} W_i Q_i \quad (7)$$

Specifically, Q_i denotes the membership degree of indicator *i*, *n* represents the number of soil indicators, and W_i is the weight of indicator *i* [59]. The SQI value was used to characterize soil microhabitat quality, with higher values indicating superior microhabitat conditions [1].

4.3. Statistical Analysis

Descriptive statistics were performed using SPSS Statistics 19.0 (IBM Corporation, Armonk, NY, USA) to characterize the distribution of stem density, diameter at breast height (DBH), tree height, aboveground biomass, and belowground biomass of *C. lanceolata* and *Q. fabri* within each diameter class. Levene's test was used to assess homogeneity of variances, and Duncan's honest significant difference (HSD) test was applied for post hoc multiple comparisons ($p < 0.05$). Pearson's correlation analysis was conducted to evaluate relationships among soil physicochemical properties and enzyme activities ($p < 0.05$). Principal component analysis (PCA; see Section 4.2.3) was used to determine the communal variance of soil indicators for SQI calculation. Principal coordinate analysis (PCoA) was conducted to ordinate differences in soil quality among diameter classes. A random forest model was employed to quantify the explanatory power of tree biomass (aboveground and belowground) for SQI variation. Data visualization was performed using Origin 2024 (OriginLab Corporation, Northampton, MA, USA).

5. Conclusions

Tree biomass–soil coupling sustains soil functioning in subtropical forests but varies with diameter class and species. This study demonstrated that diameter class-dependent tree–soil interactions varied between *C. lanceolata* and *Q. fabri*, with within-species soil

physicochemical properties and enzyme activities differing across diameter classes. In *C. lanceolata*, soil organic matter, total nitrogen, and most enzyme activities exhibited a "decrease-then-increase" pattern, reaching minima at Class III. In *Q. fabri*, these parameters generally increased with diameter class, peaking at Classes IV–V. Forest type, diameter class, and their interaction significantly influenced soil pH, total nitrogen, and enzyme activities. PCA identified diameter class as a primary driver of soil differentiation, with distinct shifts at Class III for *C. lanceolata* and Class I for *Q. fabri*. The interaction between diameter class and forest type affected SQI ($p < 0.01$): *Q. fabri* had higher SQI than *C. lanceolata* at Class V, whereas *C. lanceolata* had higher SQI than *Q. fabri* at Class I. Random forest models quantified biomass importance for SQI (test $R^2 > 0.75$): aboveground biomass contributed more in *C. lanceolata* (feature weight = 0.57) and belowground biomass in *Q. fabri* (feature weight = 0.52). These findings reveal that tree–soil feedback are mediated by both ontogenetic stage and species identity, providing a mechanistic framework for diameter- and species-specific management in subtropical forest restoration.

Supplementary Materials: The following supporting information can be downloaded at: https://www.mdpi.com/article/10.3390/plants15030402/s1, Figure S1. *C. lanceolata* plot; Figure S2. *Q. fabri* plots; Figure S3. Site Description; Table S1. Distribution characteristics of *C. lanceolata* and *Q. fabri* in different classes; Table S2. Results of one-way ANOVA for soil physical and chemical properties across diameter classes in *C. lanceolata* and *Q. fabri* forests. Table S3. Results of one-way ANOVA for oil enzyme activities across diameter classes in *C. lanceolata* and *Q. fabri* forests. Table S4. Results of one-way ANOVA for soil nutrient indicators across diameter classes in *C. lanceolata* and *Q. fabri* forests.

Author Contributions: G.L. envisioned and wrote the manuscript. Y.Y., W.L. and T.C. did the experimental work, which was supervised by L.Q. All authors contributed to the article and approved the submitted version. All authors have read and agreed to the published version of the manuscript.

Funding: This study was supported by the project "Regulation Technology of Key Substance Migration Processes at the Interface of Low-quality and Inefficient Forests in the Low Hilly Region of Southern China" (No. 2022YFF1303004).

Data Availability Statement: The original contributions presented in this study are included in the article/Supplementary Material. Further inquiries can be directed to the corresponding author.

Conflicts of Interest: The authors declare no conflict of interest.

References

1. Li, J.; Chen, T.; Zhang, M.; Shen, Y.F.; Zeng, L.X.; Xiao, W.F.; Cheng, R.M. Tree Biomass Improves Soil Microhabitat in *Pinus massoniana* Forests of Central China. *J. Soil Sci. Plant Nutr.* **2025**, *25*, 1871–1884. [CrossRef]
2. Hu, M.; Shi, H.; He, R.; Wang, N.N.; Han, Y.Z.; Dang, H.S.; Zhang, Q.F. Tree biomass allocation is governed by allometry but modulated by optimization. *For. Ecosyst.* **2025**, *15*, 100405. [CrossRef]
3. Liu, Q.Q.; Huang, Z.J.; Zou, X.H.; Ma, X.Q.; Liu, B. Adaptation strategies of *Cunninghamia lanceolata* seedlings to light intensity gradients based on morpho-physiological trade-offs. *Front. Plant Sci.* **2025**, *16*, 1646842. [CrossRef]
4. Kadowaki. Forest tree community ecology and plant-soil feedback: Theory and evidence. *Ecol. Res.* **2025**, *39*, 257–272. [CrossRef]
5. Jiang, Y.; Zang, R.G.; Lu, X.H.; Huang, Y.F.; Ding, Y.; Liu, W.D.; Long, W.X.; Zhang, J.Y.; Zhang, Z.D. Effects of soil and microclimatic conditions on the community-level plant functional traits across different tropical forest types. *Plant Soil* **2015**, *390*, 351–367. [CrossRef]
6. Dai, L.; Feng, Y.X.; Luo, G.P.; Li, Y.Z.; Xu, W.Q. The relationship between soil, climate and forest development in the mid-mountain zone of the Sangong River watershed in the northern Tianshan Mountains, China. *J. Arid. Land.* **2014**, *7*, 63–72. [CrossRef]
7. Yu, Y.C.; Yang, J.Y.; Zeng, S.C.; Wu, D.M.; Jacobs, D.F.; Sloan, J.L. Soil pH, organic matter, and nutrient content change with the continuous cropping of *Cunninghamia lanceolata* plantations in South China. *J. Soils Sediments* **2017**, *17*, 2230–2238. [CrossRef]
8. Chodak, M.; Niklińska, M. Effects of texture and tree species on microbial properties of mine soils. *Appl. Soil Ecol.* **2010**, *46*, 268–275. [CrossRef]
9. Wang, G.M.; Chen, J.; Zhu, Y.Y. Distinct bacterial community compositions in the *Populus* rhizosphere under three types of organic matter input across different soil types. *Plant Soil* **2021**, *470*, 51–63. [CrossRef]

10. Cui, Y.; Luo, F.L.; Chen, Y.H.; Zhang, M.X.; Yu, F.H. Rhizodeposition and litter decomposition of *Phragmites australis* play important roles in composition and properties of soil dissolved organic matter. *Ecol. Indic.* **2022**, *142*, 109275. [CrossRef]
11. Lu, X.H.; Zang, R.G.; Ding, Y.; Huang, J.H. Changes in biotic and abiotic drivers of seedling species composition during forest recovery following shifting cultivation on Hainan Island, China. *Biotropica* **2016**, *48*, 758–769. [CrossRef]
12. Zhang, H.; Xu, D.; Yuan, T.H.; Yang, L. Seasonal Dynamics of C:N:P Stoichiometry in Tree-Soil Systems: Nutrient Competition and Adaptation Strategies of Four Deciduous Broadleaf Species in Northeast China. *Forests* **2025**, *16*, 540. [CrossRef]
13. Li, Z.J.; Reichel, R.; Li, Z.M.; Yang, K.J.; Zhang, L.; Tan, B.; Yin, R.; Zhao, K.R.; Xu, Z.F. Effects of snow absence on available N pools and enzyme activities within soil aggregates in a spruce forest on the eastern Tibetan Plateau. *Soil Ecol. Lett.* **2021**, *4*, 376–382. [CrossRef]
14. Shen, Y.F.; Li, J.; Chen, F.F.; Cheng, R.M.; Xiao, W.F.; Wu, L.C.; Zeng, L.X. Correlations between forest soil quality and aboveground vegetation characteristics in Hunan Province, China. *Front. Plant Sci.* **2022**, *13*, 1009109. [CrossRef]
15. Yang, Y.J.; Xia, W.; Fan, Y.X.; Chong, Y.J.; Xiong, J.T.; Yu, W.J. Restoring Subtropical Forests: Alleviating P Limitation and Introducing C Limitation Using Evergreen Broad-Leaved Tree Species. *Forests* **2024**, *15*, 568. [CrossRef]
16. Ross, C.W.; Watt, M.S.; Parfitt, R.L.; Simcock, R.; Dando, J.; Coker, G.; Clinton, P.W.; Davis, M.R. Soil quality relationships with tree growth in exotic forests in New Zealand. *For. Ecol. Manag.* **2009**, *258*, 2326–2334. [CrossRef]
17. Moktan, L.; Hofmeister, J.; Oulehle, F.; Urban, O.; Hruska, J.; Metok, M.S.; Mikoláš, M.; Markuljaková, K.; Svoboda, M. Forest management reduces soil carbon sequestration potential in European temperate forests. *For. Ecol. Manag.* **2025**, *578*, 122493. [CrossRef]
18. Wu, X.F.; Yan, X.Y.; Liu, X.M.; Guo, T.Q.; Ju, C.Y.; Huang, M.B. A comparison of water use strategies between pure and mixed forests on the Chinese Loess Plateau. *Funct. Ecol.* **2025**, *40*, 256–279. [CrossRef]
19. Zhou, L.L.; Li, S.B.; Jia, Y.Y.; Heal, K.V.; He, Z.M.; Wu, P.F.; Ma, X.Q. Spatiotemporal distribution of canopy litter and nutrient resorption in a chronosequence of different development stages of *Cunninghamia lanceolata* in southeast China. *Sci. Total Environ.* **2021**, *762*, 143153. [CrossRef]
20. Li, X.G.; Xiao, J.; Salam, M.M.A.; Chen, G.C. Evaluation of dendroremediation potential of ten *Quercus* spp. for heavy metals contaminated soil: A three-year field trial. *Sci. Total Environ.* **2022**, *851*, 158232. [CrossRef]
21. Pavlin, J.; Nagel, T.A.; Svitok, M.; Di Filippo, A.; Mikac, S.; Keren, S.; Dikku, A.; Toromani, E.; Panayotov, M.; Zlatanov, T. Pathways and drivers of canopy accession across primary temperate forests of Europe. *Sci. Total Environ.* **2023**, *906*, 167593. [CrossRef] [PubMed]
22. Zhao, J.D.; Liu, X.; Wang, L.; Feng, Q.H.; Gou, C.; Bai, J.H.; Yang, X.H. Spatial distribution patterns of dominant tree species and their associations with soil factors in subalpine secondary forests of western Sichuan. *Plants* **2025**, *14*, 3424. [CrossRef] [PubMed]
23. Lian, J.S.; Cai, K.K.; Yin, A.J.; Yuan, Y.; Zhang, X.N.; Xu, C.Y. Both light and soil moisture affect the rhizosphere microecology in two oak species. *Front. Microbiol.* **2025**, *16*, 1506558. [CrossRef] [PubMed]
24. Jiang, Q.; Lin, C.F.; Guo, R.Q.; Xiong, D.C.; Yao, X.D.; Wang, X.H.; Chen, T.T.; Jia, L.Q.; Wu, D.M.; Fan, A.L. Root nitrogen uptake capacity of Chinese fir enhanced by warming and nitrogen addition. *Tree Physiol.* **2022**, *43*, 31–46. [CrossRef]
25. Zhi, K.X.; Guan, X.; Li, R.S.; Wang, J.; Duan, X.; Chen, B.-H.; Zhang, W.-D.; Yang, Q.-P. Responses of nitrogen and phosphorus resorption of understory plants to microscale soil nutrient heterogeneity in Chinese fir forests. *Chin. J. Appl. Ecol.* **2023**, *34*, 1187–1193. [CrossRef]
26. Meister, A.; Böhm, K.; Gutiérrez-Ginés, M.J.; Gaw, S.; Dickinson, N.; Robinson, B. Effects of native plants on nitrogen cycling microorganisms in soil. *Appl. Soil Ecol.* **2023**, *191*, 105031. [CrossRef]
27. Saha, S.; Huang, L.; Khoso, M.A.; Wu, H.B.; Han, D.H.; Ma, X.; Poudel, T.R.; Li, B.; Zhu, M.R.; Lan, Q.R. Fine root decomposition in forest ecosystems: An ecological perspective. *Front. Plant Sci.* **2023**, *14*, 1277510. [CrossRef]
28. Yu, Y.H.; Li, Y.T.; Wang, J.X.; Song, Y.P. Leaf-litter-soil stoichiometry and carbon and nitrogen isotopes of plant communities in dolomite district in Guizhou Province. *Acta Ecol. Sin.* **2022**, *42*, 3356–3365. [CrossRef]
29. Liu, J.W.; Liu, S.M.; Fang, X.M.; Hu, X.F.; Guo, X.M.; Zhang, L. Effects of nitrogen addition and warming on litter decomposition and C, N and P stoichiometric characteristics of Chinese fir. *Chin. J. Ecol.* **2020**, *39*, 2842–2850. [CrossRef]
30. Xu, Z.H.; Wang, Z.W.; Zhang, X.S. Mapping the forest litterfall mercury deposition in China. *Sci. Total Environ.* **2022**, *839*, 156288. [CrossRef]
31. Kyaschenko, J.; Clemmensen, K.E.; Hsienbo, A.; Karlun, E.; Lindahl, B.D. Shift in fungal communities and associated enzyme activities along an size gradient of managed *Pinus sylvestris* stands. *ISME J.* **2017**, *11*, 863–874. [CrossRef] [PubMed]
32. Zhu, X.Y.; Fang, X.; Wang, L.F.; Xiang, W.H.; Alharbi, H.A.; Lei, P.F.; Kuzyakov, Y. Regulation of soil phosphorus availability and composition during forest succession in subtropics. *For. Ecol. Manag.* **2022**, *502*, 119706. [CrossRef]
33. Obade, V.D.P.; Lal, R. A standardized soil quality index for diverse field conditions. *Sci. Total Environ.* **2016**, *541*, 424–434. [CrossRef] [PubMed]
34. Zhang, L.; Chen, Y.J.; Hao, G.Y.; Ma, K.P.; Bongers, F.; Sterck, F. Conifer and broadleaved trees differ in branch allometry but maintain similar functional balances. *Tree Physiol.* **2020**, *40*, 511–519. [CrossRef]

35. Wang, X.M.; Wang, X.P. Hotter drought and trade-off between fast and slow growth strategies as major drivers of tree-ring growth variability of global conifers. *J. Ecol.* **2022**, *112*, 1123–1139. [CrossRef]
36. Wang, B.C.; Han, Y.Y.; Sun, H.G.; He, G.X. Self-thinning line of mixed forests of *Cunninghamia lanceolata* and broad-leaved tree species. *For. Res.* **2024**, *37*, 1–12.
37. Fu, Y.H.; Yu, L.F.; Huang, Z.S. Fine root decomposition of the different root in underground habitats in Karst area. *J. For. Eng.* **2015**, *29*, 27–31. [CrossRef]
38. Miralles, I.; Domingo, F.; Cantón, Y.; Trasar-Cepeda, C.; Leirós, M.C.; Gil-Sotres, F. Hydrolase enzyme activities in a successional gradient of biological soil crusts in arid and semi-arid zones. *Soil Biol. Biochem.* **2012**, *53*, 124–132. [CrossRef]
39. Tedersoo, L.; Bahram, M.; Zobel, M. How mycorrhizal associations drive plant population and community biology. *Science* **2020**, *367*, eaba1223. [CrossRef]
40. Norris, C.E.; Hogg, K.E.; Maynard, D.G.; Curran, M.P. Stumping trials in British Columbia—organic matter removal and compaction effects on tree growth from seedlings to rotation stands. *Can. J. For. Res.* **2014**, *44*, 1402–1418. [CrossRef]
41. Nongbri, L.B.; Barik, S.K. Patterns of nitrogen resorption efficiency among different functional groups of trees in a subtropical forest of Meghalaya. *Trop. Ecol.* **2020**, *61*, 13–20. [CrossRef]
42. Peng, C.; Tu, J.; Yang, M.; Meng, Y.; Li, M.Q.; Ai, W.S. Root stoichiometric dynamics and homeostasis of invasive species *Phyllostachys edulis* and native species *Cunninghamia lanceolata* in a subtropical forest in China. *J. For. Res.* **2021**, *32*, 2001–2010. [CrossRef]
43. Fang, X.; Lin, T.; Zhang, B.Y.; Lai, Y.R.; Chen, X.P.; Xiao, Y.X.; Xie, Y.Q.; Zhu, J.M.; Yang, Y.S.; Wang, J. Regulating carbon and water balance as a strategy to cope with warming and drought climate in *Cunninghamia lanceolata* in southern China. *Front. Plant Sci.* **2022**, *13*, 1048930. [CrossRef] [PubMed]
44. Frost, I.; Rydin, H. Spatial pattern and size distribution of the animal-dispersed tree *Quercus robur* in two spruce-dominated forests. *Ecoscience* **2000**, *7*, 38–44. [CrossRef]
45. Chen, S.; Wang, C.L.; Ren, Y.C.; Zhang, H.F.; Zhou, D.D.; Li, J.; Song, H.J.; Yang, X.Q. Spatial autocorrelation patterns and influencing factors of tree growth in the secondary Picea forest in Guandi Mountains, northern China. *Acta Ecol. Sin.* **2023**, *43*, 1572–1583. [CrossRef]
46. *GB/T 43648-2024*; State Forestry and Grassland Administration of the People's Republic of China. Tree Biomass Models and Related Parameters to Carbon Accounting for Major Tree Species. Standards Press of China: Beijing, China, 2024. Available online: https://www.forestry.gov.cn/c/www/kjkjxw/555638.jhtml (accessed on 14 December 2025).
47. Bao, S.D. Soil and agricultural chemistry analysis. In *Soil and Agricultural Chemistry Analysis*; China Agricultural Press: Beijing, China, 2000; pp. 25–239.
48. Johnsen, A.R.; Jacobsen, O.S. A quick and sensitive method for the quantification of peroxidase activity of organic surface soil from forests. *Soil Biol. Biochem.* **2008**, *40*, 814–821. [CrossRef]
49. Najdovski, B.; Djuric, S.; Pekec, S.; Milovic, M.; Orlovic, S.; Pilipovic, A. Impact of systematic groups of microorganisms on dehydrogenase activity in soils within *Quercetum montanum* typicum forest community. *Forests* **2025**, *16*, 322. [CrossRef]
50. Jiang, D.Q.; Wu, C.R.; Jiang, N.; Qiu, W.W.; Chen, L.J.; Zhang, Y.L.; Chen, Z.H. Urease inhibitors increased soil intracellular urease activity while altering the *ureC* gene abundance and community structure in red soil. *Appl. Soil Ecol.* **2025**, *206*, 105908. [CrossRef]
51. Miao, S.J.; Wu, X.Y.; Guo, Y.; Zhao, H.F.; Qiao, Y.F. Different responses of enzyme activities to 6-year warming after transplant of the 12 types of soils. *J. Plant Nutr. Soil Sci.* **2022**, *186*, 487–494. [CrossRef]
52. Xiao, S.H.; You, H.M.; You, W.B.; Liu, J.S.; Cai, C.T.; Wu, J.Q.; Ji, Z.R.; Zhan, S.H.; Hu, Z.S.; Zhang, Z.R. Rhizosphere and bulk soil enzyme activities in a *Nothotsuga longibracteata* forest in the Tianbaoyan National Nature Reserve, Fujian Province, China. *J. For. Res.* **2016**, *28*, 521–528. [CrossRef]
53. Li, W.Q.; Huang, Y.X.; Chen, F.S.; Liu, Y.Q.; Lin, X.F.; Zong, Y.Y.; Wu, G.Y.; Yu, Z.R.; Fang, X.M. Mixing with broad-leaved trees shapes the rhizosphere soil fungal communities of coniferous tree species in subtropical forests. *For. Ecol. Manag.* **2021**, *480*, 118664. [CrossRef]
54. Huang, Z.J.; Selvaraj, S.; Duraisamy, V.; Liu, Q.Q.; Cheng, H.; Guo, F.T.; Ma, X.Q. Identification of indicators for evaluating and monitoring the effects of Chinese fir monoculture plantations on soil quality. *Ecol. Indic.* **2018**, *93*, 547–554. [CrossRef]
55. Feng, J.Y.; Chu, S.S.; Wang, J.; Wu, D.M.; Mo, Q.F.; Zeng, S.C. Comprehensive evaluation of soil fertility of five typical forest stands in south China. *J. South China Agric. Univ.* **2018**, *39*, 73–81. [CrossRef]
56. Masto, R.E.; Chhonkar, P.K.; Singh, D.; Patra, A.K. Alternative soil quality indices for evaluating the effect of intensive cropping, fertilisation and manuring for 31 years in the semi-arid soils of India. *Environ. Monit. Assess.* **2008**, *136*, 419–435. [CrossRef]
57. Fu, L.C.; Ding, Z.J.; Tang, M.; Zeng, H.; Zhu, B. Seasonal dynamics of activities, temperature sensitivities and vector characteristics of extracellular enzymes in rhizosphere and bulk soils of two temperate forests in Mt. Dongling, Beijing. *Acta Sci. Nat. Univ. Pekin.* **2022**, *58*, 503–516. [CrossRef]

58. Chen, C.; Chen, H.Y.H.; Chen, X.L.; Huang, Z.Q. Meta-analysis shows positive effects of plant diversity on microbial biomass and respiration. *Nat. Commun.* **2019**, *10*, 1332. [CrossRef]
59. Rahmanipour, F.; Marzaioli, R.; Bahrami, H.A.; Fareidouni, Z.; Bandarabadi, S.R. Assessment of soil quality indices in agricultural lands of Qazvin Province. *Iran. Ecol. Indic.* **2014**, *40*, 19–26. [CrossRef]

Disclaimer/Publisher's Note: The statements, opinions and data contained in all publications are solely those of the individual author(s) and contributor(s) and not of MDPI and/or the editor(s). MDPI and/or the editor(s) disclaim responsibility for any injury to people or property resulting from any ideas, methods, instructions or products referred to in the content.